Vegetation dynamics and rainfall sensitivity of the Amazon

Thomas Hilker[a,1], Alexei I. Lyapustin[b], Compton J. Tucker[b], Forrest G. Hall[b,c], Ranga B. Myneni[d], Yujie Wang[b,c], Jian Bi[d], Yhasmin Mendes de Moura[e], and Piers J. Sellers[b]

[a]College of Forestry, Corvallis, OR 97331; [b]Goddard Space Flight Center, NASA, Greenbelt, MD 20771; [c]Joint Center for Earth System Technology, University of Maryland Baltimore County, Baltimore, MD 21228; [d]Department of Earth and Environment, Boston University, Boston, MA 02215; and [e]Divisão de Sensoriamento Remoto, Instituto Nacional de Pesquisas Espaciais, São José dos Campos, 12245-970 São Paulo State, Brazil

We show that the vegetation canopy of the Amazon rainforest is highly sensitive to changes in precipitation patterns and that reduction in rainfall since 2000 has diminished vegetation greenness across large parts of Amazonia. Large-scale directional declines in vegetation greenness may indicate decreases in carbon uptake and substantial changes in the energy balance of the Amazon. We use improved estimates of surface reflectance from satellite data to show a close link between reductions in annual precipitation, El Niño southern oscillation events, and photosynthetic activity across tropical and subtropical Amazonia. We report that, since the year 2000, precipitation has declined across 69% of the tropical evergreen forest (5.4 million km^2) and across 80% of the subtropical grasslands (3.3 million km^2). These reductions, which coincided with a decline in terrestrial water storage, account for about 55% of a satellite-observed widespread decline in the normalized difference vegetation index (NDVI). During El Niño events, NDVI was reduced about 16.6% across an area of up to 1.6 million km^2 compared with average conditions. Several global circulation models suggest that a rise in equatorial sea surface temperature and related displacement of the intertropical convergence zone could lead to considerable drying of tropical forests in the 21st century. Our results provide evidence that persistent drying could degrade Amazonian forest canopies, which would have cascading effects on global carbon and climate dynamics.

Amazon | climate change | precipitation | NDVI | MODIS | MAIAC

Rise in equatorial sea surface temperature has led to concerns that intensified El Niño southern oscillation (ENSO) events and a displacement of the intertropical convergence zone (1) could alter precipitation patterns in Amazonia (2, 3), resulting in increased length of the dry season (4) and more frequent severe droughts (5, 6). The feedbacks of such drying on global climate change could be substantial; the Amazon rainforest stores an estimated 120 billion tons of carbon (7, 8). Loss of forest productivity across Amazonia would clearly exacerbate atmospheric CO_2 levels (9, 10); however, the extent to which drying affects terrestrial vegetation is currently unknown (11). Satellite remote sensing is the only practical way to observe the potential impacts that these changes may have on vegetation at useful spatial and temporal scales (12), but in recent years, conflicting results have been reported of whether productivity of tropical forests is limited by sunlight or precipitation (7, 11, 13–16). Several studies have indicated that gross primary productivity increases initially during drought as a result of an increase in photosynthetically active radiation (PAR) (17, 18), but sensitivity to prolonged drought events and thresholds of forest dieback remain unclear. For instance, as a result of the severe Amazon drought in 2005, Phillips et al. (8) estimated an accumulated carbon loss of 1.2–1.6 petagram (Pg) based on records from 55 long-term monitoring plots. In contrast, Saleska et al. (13) reported greening of the Amazon forest based on remotely sensed estimates of the enhanced vegetation index acquired from the Moderate Resolution Imaging Spectroradiometer (MODIS) from the National Aeronautics and Space Administration (NASA). Saleska et al. (13) concluded that tropical forests were more drought resistant than previously thought and remained a strong carbon sink even during drought. However, these assertions were subsequently questioned (7, 11), and after a second drought in 2010, Xu et al. (19) documented widespread decline in tropical vegetation.

Similar to interannual changes related to drought, there have also been contradictory findings related to seasonal changes between dry and wet seasons. A substantial body of literature (15, 17, 18, 20–22) supports the view that photosynthetic activity increases during the dry season in response to an increase in incident PAR, whereas water supply is maintained through deep root systems of tropical forests (23). In contrast, Morton et al. (14) argued that MODIS-derived observations of seasonal greening of tropical vegetation are an artifact of the sun-sensor geometry, concluding that tropical forests maintain consistent greenness throughout the dry and wet seasons.

Resolving the discussion about drought tolerance of tropical vegetation is critical to reduce uncertainties in carbon balance models (16, 24, 25) and establish possible thresholds beyond which forest dieback may occur (15). Recent work suggests a substantial uncertainty of MODIS surface reflectance across the Amazon basin as a likely cause of these discrepancies in interpretation (26–28). Surface reflectance is routinely derived from top of atmosphere measurements using pixel-based atmospheric correction and cloud screening (29). Poor estimation of atmospheric aerosol loadings (11, 26) and deficiencies in cloud screening (30) can, therefore, introduce errors in vegetation indices (27). We take advantage of a new multiangle implementation of

Significance

Understanding the sensitivity of tropical vegetation to changes in precipitation is of key importance for assessing the fate of the Amazon rainforest and predicting atmospheric CO_2 levels. Using improved satellite observations, we reconcile observational and modeling studies by showing that tropical vegetation is highly sensitive to changes in precipitation and El Niño events. Our results show that, since the year 2000, the Amazon forest has declined across an area of 5.4 million km^2 as a result of well-described reductions in rainfall. We conclude that, if drying continues across Amazonia, which is predicted by several global climate models, this drying may accelerate global climate change through associated feedbacks in carbon and hydrological cycles.
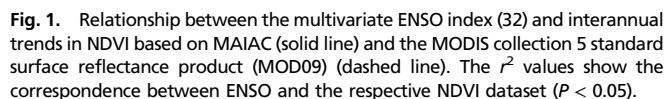
Fig. 1. Relationship between the multivariate ENSO index (32) and interannual trends in NDVI based on MAIAC (solid line) and the MODIS collection 5 standard surface reflectance product (MOD09) (dashed line). The r^2 values show the correspondence between ENSO and the respective NDVI dataset ($P < 0.05$).

atmospheric correction algorithm (MAIAC) (31) to refine the analysis of the sensitivity of tropical and subtropical vegetation to variation in precipitation using daily observations of MODIS surface reflectance acquired between 2000 and 2012. MAIAC improves the accuracy of satellite-based surface reflectance over tropical vegetation by 3- to 10-fold compared with current MODIS products (30). This improvement is accomplished, in part, through a more accurate and less conservative cloud mask, which increases the number of clear-sky observations by a factor of 2–5 compared with standard procedures (30). A higher number of clear-sky observations is particularly important for analysis of tropical regions, where average cloud cover may be as high as 70% during the dry season and 95–99% during the wet season (30). This improvement along with the removal of calibration errors in the latest MODIS Terra Collection 6 (C6) data provide us with more confidence in interpreting the state and changes in the Amazon forests.

Results

Inter- and Intraannual Vegetation Dynamics. Fig. 1 and Fig. S1 compare interannual changes in normalized difference vegetation index (NDVI) with the multivariate ENSO index from the National Oceanic and Atmospheric Administration (32); vegetation browning and greening are defined as total area of Amazon rainforest (in million kilometers^2) with net annual changes in NDVI greater than the SD of the annual means. Our results show a close correspondence between satellite-observed changes in NDVI and ENSO patterns ($r^2 = 0.35$, $P < 0.05$). Strong positive departures from the long-term ENSO mean led to significant reductions in greenness across large parts of the Amazon basin during El Niño events. Similarly, years with above-average precipitation resulted in increased greening during La Niña cycles (Fig. S1). ENSO patterns affected large areas of vegetation; between both ENSO extremes, NDVI was reduced across more than 1.5 million km^2, which corresponds to 30% of the entire basin. The relationship between NDVI and ENSO cannot be explained by reduced cloud contamination during drier years; such artifacts would be expected to show opposite trends in the vegetation index (33). Validation of changes observed over such large extents is difficult; however, some confidence in remotely sensed data can be obtained by comparing NDVI values with existing field measurements of leaf area index (Fig. S2). We emphasize that the relationship between NDVI and ENSO could not be observed with the C5 MODIS surface reflectance product (Fig. 1 and Fig. S1), which has been at the basis of some of the controversial findings (26). The lack of interannual variability in C5 is in agreement with previous analyses (7). In part, the monotone trends found in C5 are most likely explained by the MODIS Terra calibration degradation over time and the fact

that the standard MODIS C5 dataset relies almost exclusively on the morning Terra data because of high cloudiness in the afternoon during the Aqua overpass. MAIAC is based on MODIS C6 Level 1B (calibrated and geometrically corrected) data, which removed the major effect of calibration degradation of the sensor present in earlier collections.

Intraannual changes in NDVI were strongly related to changes in precipitation as estimated from microwave measurements as part of the Tropical Rainfall Measurement Mission (TRMM) of NASA. Fig. 2A shows dry season greening as obtained from changes in monthly mean NDVI at the beginning and the end of the dry season (April and October). Monthly means were obtained from data collected between 2000 and 2012 and excluded the extreme drought years of 2005 and 2010 (5, 6). Greening of tropical forest was negatively related to precipitation estimates derived from TRMM (Fig. 2B), suggesting that, on average, photosynthetic activity was higher during drier months than wetter months (22). Statistically significant ($P < 0.05$) relationships between δNDVI and δprecipitation were particularly strong in the southern Amazon, where differences between dry and wet seasons are pronounced (34). In sharp contrast, the relationship between changes in precipitation and adjacent savannah grasslands was positive, suggesting an enhancement of photosynthetic activity during the wet season.

Net Changes Observed Between 2000 and 2012. Overall, there was a net decline in precipitation across much of the eastern and southeastern part of the Amazon basin and bordering subtropical grasslands, where rainfall was reduced by up to 25% between 2000 and 2012 (Fig. 3A). Independent observations of changes in terrestrial water storage (TWSC), which were based on the Global Land Data Assimilation System and satellite observations from the Gravity Recovery and Climate Experiment (35), confirmed a coincident depletion by up to 10 cm water across the same area (Fig. 3B). On average, about 7.5 more d with cloud-free observations occurred in 2012 compared with 2000 based on the MAIAC cloud mask, which is in agreement with previous reports (4). Statistically significant ($P < 0.05$) net changes in mean annual NDVI are shown in Fig. 3C. In particular, vegetation greenness declined across the southeastern part of the Amazon forest. In our analysis on trends in NDVI, we were careful to exclude areas that underwent changes in land cover (36). We examined vegetation decline by fitting a time-series model (37) to describe variations in NDVI for each 1-km grid cell (Fig. S3). This approach allowed us to model changes in NDVI continuously between 2000 and 2012, with a mean SE of 0.024 (SE < 0.015 for the tropical evergreen forest).
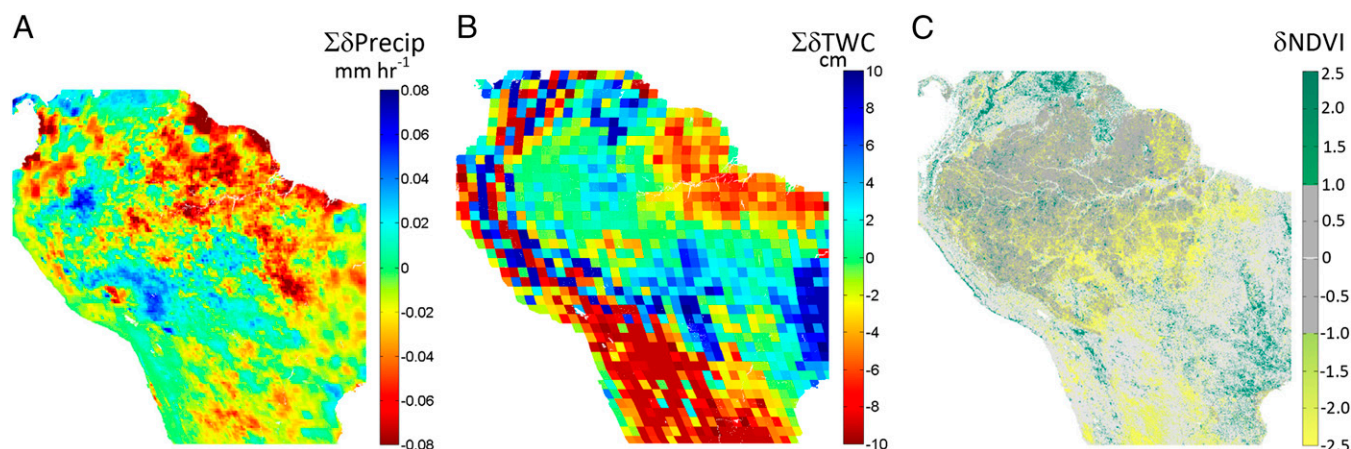

Fig. 2. (A) Dry season greening ($P < 0.05$) of the Amazon forests and (B) precipitation relationships (correlation coefficient; $P < 0.05$) of Amazon forests and grassland savannahs. Monthly estimates were averaged between 2000 and 2012 but exclude the drought years of 2005 and 2010. Estimates of NDVI were normalized to a nadir view and a solar zenith angle of 45°.

Hilker et al.
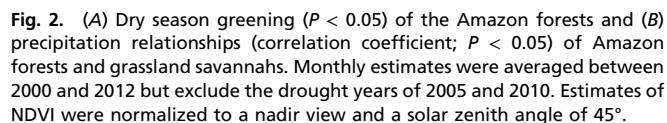
Fig. 3. Net changes in (*A*) monthly precipitation (millimeter hour^{-1}) and (*B*) TWSC (centimeter) and (*C*) normalized change in annual NDVI normalized by its SD between 2000 and 2012.

Fig. 4 shows monthly averaged changes in NDVI for the dominant land cover types (36) separated by regions with net declines in precipitation (Fig. 4 *A–C*) and regions where precipitation remained unchanged or increased (Fig. 4 *D–F*). Of the tropical evergreen forest, 69.4% (5.4 million km^2) recorded a net decrease in precipitation of, on average, 16.6% (Fig. 4*A*), whereas rainfall remained the same or increased across 30.6% (2.8 million km^2) of the area between 2000 and 2012. The decrease in precipitation accounted for about 55% of the observed decline in NDVI. Although the size of this decline was small (0.8%), the implications could be considerable, because the trend has been observed over 13 y and across an area of 5.4 million km^2. For comparison, the estimated 1 billion tons carbon released during the 2005 drought (8) corresponds to an 8% reduction of satellite-observed NDVI below the seasonal mean but only across an area of 0.32 million km^2 (19) (Figs. S4 and S5).
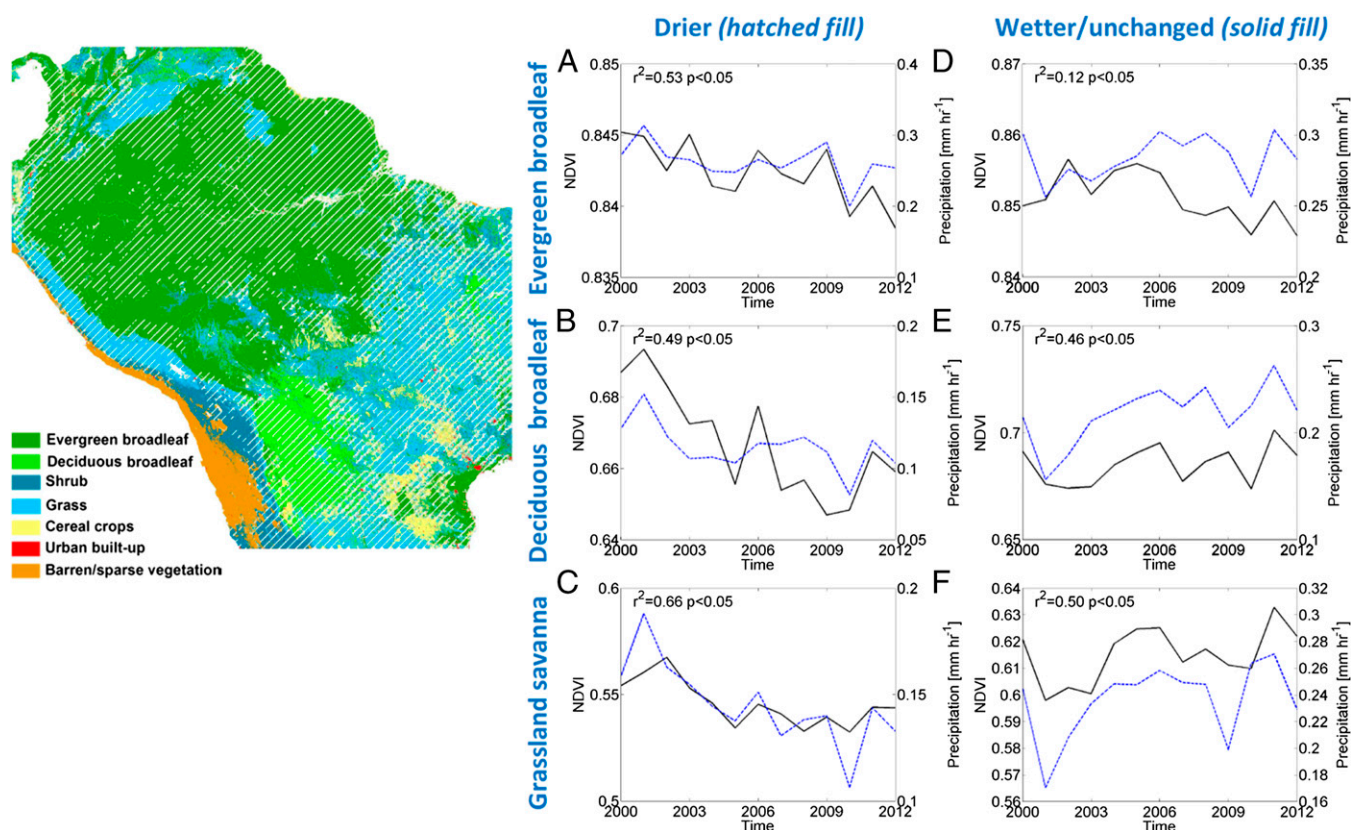
Fig. 4. Changes in NDVI and precipitation by land cover. Land cover types are derived from the MOD12Q1 MODIS product (36); only the most important types are shown. Areas with solid fill became wetter or remained unchanged, and hatched areas showed a net decrease in precipitation. *A–F* show mean annual NDVI (black solid line; left axis) and mean annual precipitation (blue dashed line; right axis) for the three major land cover types separated for (*A–C*) areas with a net decrease in precipitation and (*D–F*) areas with net increase or unchanged precipitation rates. The *r*^{2} is derived from the linear regression of NDVI and precipitation.

The 2010 drought, which spread across 1.68 million km^2 in the southeastern part (19), resulted in 5% reduction in NDVI (5). In both of these cases, decline in canopy greenness was limited to a much shorter period (Fig. S4) than the changes shown in Fig. 4A. Although vegetation decline after reductions in precipitation was evident, increase in precipitation did not necessarily result in an increase in greenness (Fig. 4 D and E).

In addition to tropical evergreen forest, precipitation was also reduced across about 80% of the deciduous forest (1.4 million km^2) and adjacent grassland savannah (3.3 million km^2) by, on average, about 25% and 30%, respectively (Fig. 4 B and C). Net decrease in precipitation accounted for between 49% (deciduous broadleaf) and 66% (grassland savanna) of the decline in vegetation greenness. An average decline of about 4% (Fig. 4B) occurred across drier deciduous broadleaf vegetation, whereas NDVI in the drier grassland savannas decreased by about 7% between 2000 and 2012 (Fig. 4C).

Discussion

Although increased PAR during the dry season may initially enhance productivity of tropical vegetation (15, 18, 22), sustained drought may reduce photosynthesis and canopy leaf area and ultimately, cause tree mortality (8, 13, 38). Our research contributes to the recent discussion on drought sensitivity of Amazon forests (11, 13, 14, 21, 22) in two ways: (i) it helps reconcile results from field and modeling studies with remote sensing observations, something that, so far, has been challenging (26, 39), and (ii) it provides a sounder basis for concluding that tropical vegetation has declined as a result of reductions in precipitation across large parts of Amazonia since 2000. The implication of the latter is that a large net increase in the release of CO$_2$ to the atmosphere may have occurred as a result of recent drying, particularly in eastern and southeastern Amazonia (40). Similar observational evidence reported for the Congo basin (41) suggests that precipitation-related decline has also occurred in other tropical regions and therefore, is more widespread than previously assumed.

Reconciliation of observational and modeling studies signifies an important step to quantify carbon dynamics across vegetation and moisture gradients in Amazonia, because it helps us to better understand the underlying biophysics that control the direction and strength of fluxes from the region (39). These fluxes have significant implications for global climate change. Tian et al. (42) estimated tropical carbon feedbacks to vary between a 0.2-Pg carbon source and a 0.7-Pg carbon sink per year during El Niño/La Niña extremes. Similarly, Gatti et al. (43) estimated that, during wet years, the Amazon forest has a net carbon sink of 0.25 ± 0.14 petagram carbon per year (Pg C yr^{-1}), whereas the basin lost 0.48 ± 0.18 Pg C yr^{-1} during dry years based on atmospheric measurements from air sample profiles. Consistent with both field studies (23, 38, 43, 44) and model predictions (42, 45, 46), our results confirm a strong response of remotely sensed NDVI to El Niño/La Niña oscillations (Fig. 1). These findings are also consistent with the work by Asner et al. (47), which used spatial filtering of NDVI data to produce a regionally averaged estimate of El Niño effects on greenness and productivity. The improvement in the quality of remotely sensed data reported here allowed us to link El Niño/La Niña events to vegetation responses at a basin-wide scale, while also offering an explanation for the lack of such correlations with previous products (trends are shown in Fig. 1 and Fig. S1) (7).

Similar to interannual variability, seasonal changes in vegetation have been recognized in both measurement (17) and modeling studies (46, 48), but remote sensing of these changes has been difficult and controversial (14, 21, 22). Ground validation of remotely sensed changes in Amazon forests is often challenging, because field data are limited to a relatively small number of spatially discrete observations. Nonetheless, the results presented in Figs. S2 and S5 as well as previous findings on data quality and noise statistics (30) provide confidence in the presented change estimates.

Our results show that parts of the Amazon forest do green up during the dry season, which is consistent with previous studies indicative of light limitations during the wet season (15, 17, 18, 20–22), as long as a supply of water exists for deep-rooted trees (23). These findings cannot be explained by directional effects, because all observations have been normalized to a common sun observer geometry (31). Opposite findings based on C5 MODIS data (14) will require additional analyses to be addressed separately; one possible explanation might be noise in the C5 dataset (30), rendering residual changes below a statistical significance level. During extended droughts, because the soil water supply is drained, foliage begins to shed, and NDVI is reduced. We emphasize that neither seasonal nor interannual changes can be explained as artifacts caused by variations in sun sensor geometry (14), and also, they cannot result from atmospheric or cloud effects (26, 30), because (i) MAIAC accounts for changes in surface reflectance caused by changes in view and sun direction (31) and (ii) atmospheric loadings or cloud contamination would not be expected to cause opposite trends for different land cover types (Fig. 2). The results presented in this study contradict previous reports on drought-related greening (13); instead, they confirm large-scale dieback of the vegetation (Figs. S4 and S5) during extreme droughts (11, 19), which corresponds well to spatial patterns of field-observed changes in biomass (8). Because cloud cover is seasonally dependent, it seems plausible that previously reported increases in Amazon greenness could, at least in part, result from reduced cloudiness and reduced probability of corruption of surface reflectance (26, 30), which would cause negative artifacts on vegetation indices (33).

The last decade has seen considerable drying of eastern and southeastern Amazonia (49, 50), and more intense drought events are likely in the future (5), because subpolar melting is strengthening the sea surface temperature gradient between the north and south Atlantic, thereby shifting the intertropical convergence zone northward (51). Our study links these trends to a moderate but widespread decline of vegetation, particularly in the eastern and southeastern Amazon (Fig. 3) (52). This assertion is supported by model predictions (40) and atmospheric measurements (43), suggesting that dry season water stress is likely to increase in eastern Amazonia over the 21st century as a result of increased climate variability. The observed vegetation decline is also consistent with observed changes in TWSC and precipitation patterns (Fig. 3), closely following both trends (Figs. 1 and 4). Regionally, logging and forest conversion to pasture and fields may have also contributed to reductions in precipitation (51), particularly in the southern and eastern limits of the evergreen forest, because removal of deep-rooted trees will reduce transpiration of water to the atmosphere, thereby hindering the formation of clouds (53). Other regional differences in climatic effects may exist as a result of topography, particularly along the western edge of the basin (54).

Vegetation decline, as depicted in Figs. 3 and 4, will likely have strong implications on global climate change (55) because of the geographical extent of the observed decline, the role that tropical rainforests play in regional meteorology (56), and the magnitude of the carbon stored in tropical vegetation (57). Thirteen years of observations available from MODIS data are insufficient to attribute drying to anthropogenic sources (50) or establish long-term patterns or thresholds after which dieback might occur. However, our results show a clear response of tropical vegetation to changes in rainfall. We conclude that, if drying continues across the eastern and southeastern part of Amazonia, this drying could lead to broad degradation of tropical forests, with potentially strong implications for atmospheric CO$_2$ levels and global climate change (58).

Methods

MODIS Observations. Our study encompasses 16 MODIS tiles (h10v08 and h13v11), which is a land area of 16.75 million km^2 spanning 10° N to 30° S in latitude and 80° W to 42° W in longitude. The area is characterized by seasonal tropical savannah and seasonal deciduous forest in the north and south and tropical evergreen forest in the equatorial region. Tropical regions frequently experience high cloud cover and high variability in atmospheric aerosols because of seasonal biomass burning (59). These atmospheric conditions are challenging to assess with traditional algorithms that rely on spectral and thermal reflectance thresholds alone (30). MAIAC is a new generation cloud screening and atmospheric correction algorithm that uses an adaptive time-series analysis and processes groups of pixels to derive atmospheric aerosol and surface reflectance without typical empirical assumptions. MAIAC implements a sliding window approach, storing up to 16 d of MODIS observations gridded to 1-km resolution. These data are used to derive a spectral regression coefficient relating surface reflectance in the blue (0.466 μm) and short-wave IR (2.13 μm) for aerosol retrievals (60) and obtain parameters of surface bidirectional reflectance distribution function (61) in the MODIS reflective bands (31). Using time-series analysis over 4–16 d, MAIAC is able to separate stable surface background with its characteristic spatial pattern from generally random and changing fields of clouds (62). MAIAC also features a dynamic land–water–snow classification and change detection algorithm to account for rapid and seasonal changes in surface reflectance of the time-series data (31). Currently, MAIAC is undergoing operational code conversion and testing, and it is expected to become an operational MODIS algorithm in 2014. For this work, we used MODIS C6 Level 1B (calibrated and geometrically corrected) data, which removed major sensor calibration degradation effects present in earlier collections. Detailed descriptions of MAIAC and quality testing (31, 60) as well as an assessment of errors and uncertainties over the tropical regions (30) are provided elsewhere.

Precipitation. Monthly rainfall was obtained from the TRMM at 0.25° spatial resolution between 2000 and 2012 (3B43, version 7) (13). TRMM provides monthly estimates of precipitation in millimeter hour^{-1}. The 3B43 dataset combines microwave images with the IR-based Geostationary Operational Environmental Satellite Precipitation Index and a network of gauge data (63). Although previous research (59) has shown good agreement with independent rain gauge data in the Brazilian Amazon, rainfall is somewhat underestimated during very wet months (>300 mm mo^{-1}). TRMM data were resampled to match MODIS data at 1-km spatial resolution using a bilinear interpolation technique. Estimates of monthly precipitation (P) were normalized by subtracting the mean annual precipitation of 2000 and 2002 as baseline from monthly data (58). Net changes were then assessed by summation of the normalized changes to assess gains or losses over time,

$$\partial P = \frac{\sum_1^n \left(P - \overline{P_{2000,2002}} \right)}{n},\qquad [1]$$

where n is the total number of monthly observations. Although we recognize that the magnitude of trends will depend on the selection of the baseline, the goal of this analysis was to investigate sensitivity of vegetation to changes in precipitation rather than establish long-term drying or wetting trends. These years were selected, because they both represent non-El Niño events and therefore, fairly normal conditions. We have also tested the single year (2000) and the whole-record average baseline approach and found little effect on spatial domains of detected change.

Changes in TWSC. Changes in TWSC were obtained from the Global Data Assimilation System, a land surface modeling system that integrates data from advanced Earth-observing satellite- and ground-based observations to support and improve hydrometeorological predictions (64). Monthly TWSC estimates were obtained at 1° spatial resolution between 2000 and 2012 from the Earth Sciences Data and Information Services Center from NASA (grace.jpl.nasa.gov). Net changes in TWSC were derived analogous to changes in precipitation.

Time-Series Analysis. Time-series analysis of NDVI was used to derive trends in vegetation over time (37). Several methods exist for assessing changes in NDVI time series, including those based on simple thresholds or more comprehensive time-series models. Here, time-series fitting is based on the TIMESAT approach (37). Originally developed for the NDVI series from the Advanced Very High Resolution Imaging Spectroradiometer, the technique has been adapted for MODIS (65). The Savitzky–Golay filter method was used to fit splines to a temporally moving window of satellite observations. The use of this adaptive filtering method allows fitting of time series of observations without assuming data stationary. To take into account that most noise in NDVI is negatively biased, the algorithm was fitted to the upper envelope of the observed NDVI (37). Net changes in NDVI were obtained analogs to changes in precipitation (Eq. **1**). MODIS data before late February of 2000 were substituted with corresponding monthly averages from 2001 to 2002 to obtain a full set of observations for the year 2000.

1. Li W, Fu R, Dickinson RE (2006) Rainfall and its seasonality over the Amazon in the 21st century as assessed by the coupled models for the IPCC AR4. *J Geophys Res* 111: D02111.
2. Rammig A, et al. (2010) Estimating the risk of Amazonian forest dieback. *New Phytol* 187(3):694–706.
3. Jupp TE, et al. (2010) Development of probability density functions for future South American rainfall. *New Phytol* 187(3):682–693.
4. Fu R, et al. (2013) Increased dry-season length over southern Amazonia in recent decades and its implication for future climate projection. *Proc Natl Acad Sci USA* 110(45):18110–18115.
5. Lewis SL, Brando PM, Phillips OL, van der Heijden GM, Nepstad D (2011) The 2010 Amazon drought. *Science* 331(6017):554.
6. Marengo JA, Nobre CA, Tomasella J, Cardoso MF, Oyama MD (2008) Hydro-climate and ecological behaviour of the drought of Amazonia in 2005. *Philos Trans R Soc Lond B Biol Sci* 363(1498):1773–1778.
7. Atkinson PM, Dash J, Jeganathan C (2011) Amazon vegetation greenness as measured by satellite sensors over the last decade. *Geophys Res Lett* 38:L19105.
8. Phillips OL, et al. (2009) Drought sensitivity of the Amazon rainforest. *Science* 323(5919):1344–1347.
9. Cox PM, Betts RA, Jones CD, Spall SA, Totterdell IJ (2000) Acceleration of global warming due to carbon-cycle feedbacks in a coupled climate model. *Nature* 408(6809):184–187.
10. Fung IY, Doney SC, Lindsay K, John J (2005) Evolution of carbon sinks in a changing climate. *Proc Natl Acad Sci USA* 102(32):11201–11206.
11. Samanta A, et al. (2010) Amazon forests did not green-up during the 2005 drought. *Geophys Res Lett* 37(5):L05401.
12. Shukla J, Nobre C, Sellers P (1990) Amazon deforestation and climate change. *Science* 247(4948):1322–1325.
13. Saleska SR, Didan K, Huete AR, da Rocha HR (2007) Amazon forests green-up during 2005 drought. *Science* 318(5850):612.
14. Morton DC, et al. (2014) Amazon forests maintain consistent canopy structure and greenness during the dry season. *Nature* 506(7487):221–224.
15. Brando PM, et al. (2010) Seasonal and interannual variability of climate and vegetation indices across the Amazon. *Proc Natl Acad Sci USA* 107(33):14685–14690.
16. Davidson EA, et al. (2012) The Amazon basin in transition. *Nature* 481(7381):321–328.
17. Hutyra LR, et al. (2007) Seasonal controls on the exchange of carbon and water in an Amazonian rain forest. *J Geophys Res* 112:G03008.
18. Graham EA, Mulkey SS, Kitajima K, Phillips NG, Wright SJ (2003) Cloud cover limits net CO2 uptake and growth of a rainforest tree during tropical rainy seasons. *Proc Natl Acad Sci USA* 100(2):572–576.
19. Xu L, et al. (2011) Widespread decline in greenness of Amazonian vegetation due to the 2010 drought. *Geophys Res Lett* 38(7):L07402.
20. Samanta A, et al. (2012) Seasonal changes in leaf area of Amazon forests from leaf flushing and abscission. *J Geophys Res* 117:G01015.
21. Myneni RB, et al. (2007) Large seasonal swings in leaf area of Amazon rainforests. *Proc Natl Acad Sci USA* 104(12):4820–4823.
22. Huete AR, et al. (2006) Amazon rainforests green-up with sunlight in dry season. *Geophys Res Lett* 33:L06405.
23. Nepstad DC, et al. (1994) The role of deep roots in the hydrological and carbon cycles of Amazonian forests and pastures. *Nature* 372:666–669.
24. Pan Y, et al. (2011) A large and persistent carbon sink in the world's forests. *Science* 333(6045):988–993.
25. DeFries RS, et al. (2002) Carbon emissions from tropical deforestation and regrowth based on satellite observations for the 1980s and 1990s. *Proc Natl Acad Sci USA* 99(22):14256–14261.
26. Samanta A, Ganguly S, Vermote E, Nemani RR, Myneni RB (2012) Why is remote sensing of amazon forest greenness so challenging? *Earth Interactions* 16(7):1–14.
27. Zelazowski P, Sayer AM, Thomas GE, Grainger RG (2011) Reconciling satellite-derived atmospheric properties with fine-resolution land imagery: Insights for atmospheric correction. *J Geophys Res* 116:D18308.

28. Asner GP, Alencar A (2010) Drought impacts on the Amazon forest: The remote sensing perspective. *New Phytol* 187(3):569–578.
29. Vermote E, Kotchenova S (2008) Atmospheric correction for the monitoring of land surfaces. *J Geophys Res Atmos* 113:D23S90.
30. Hilker T, et al. (2012) Remote sensing of tropical ecosystems: Atmospheric correction and cloud masking matter. *Remote Sens Environ* 127:370–384.
31. Lyapustin A, Wang Y, Laszlo I, Hilker T (2012) Multi-Angle Implementation of Atmospheric Correction for MODIS (MAIAC). Part 3: Atmospheric correction. *Remote Sens Environ* 127:385–393.
32. Wolter K (1987) The Southern Oscillation in surface circulation and climate over the tropical Atlantic, Eastern Pacific, and Indian Oceans as captured by cluster analysis. *Journal of Climate and Applied Meteorology* 26(4):540–558.
33. Myneni R, Asrar G (1994) Atmospheric effects and spectral vegetation indices. *Remote Sens Environ* 47:390–402.
34. Marengo JA, Liebmann B, Kousky VE, Filizola NP, Wainer IC (2001) Onset and end of the rainy season in the Brazilian Amazon Basin. *J Clim* 14:833–852.
35. Syed TH, Famiglietti JS, Rodell M, Chen J, Wilson CR (2008) Analysis of terrestrial water storage changes from GRACE and GLDAS. *Water Resour Res* 44(2):W02433.
36. Friedl MA, et al. (2010) MODIS Collection 5 global land cover: Algorithm refinements and characterization of new datasets. *Remote Sens Environ* 114:168–182.
37. Jönsson P, Eklundh L (2004) TIMESAT—a program for analyzing time-series of satellite sensor data. *Comput Geosci* 30(8):833–845.
38. Brando PM, et al. (2008) Drought effects on litterfall, wood production and below-ground carbon cycling in an Amazon forest: Results of a throughfall reduction experiment. *Philos Trans R Soc Lond B Biol Sci* 363(1498):1839–1848.
39. Baker IT, et al. (2008) Seasonal drought stress in the Amazon: Reconciling models and observations. *J Geophys Res* 113:G00B01.
40. Malhi Y, et al. (2009) Exploring the likelihood and mechanism of a climate-change-induced dieback of the Amazon rainforest. *Proc Natl Acad Sci USA* 106(49):20610–20615.
41. Zhou L, et al. (2014) Widespread decline of Congo rainforest greenness in the past decade. *Nature* 509(7498):86–90.
42. Tian H, Melillo JM, Kicklighter DW (1998) Effect of interannual climate variability on carbon storage in Amazonian ecosystems. *Nature* 396:1996–1999.
43. Gatti LV, et al. (2014) Drought sensitivity of Amazonian carbon balance revealed by atmospheric measurements. *Nature* 506:76–80.
44. Williamson GB, et al. (2000) Amazonian tree mortality during the 1997 El Nino drought. *Conserv Biol* 14(5):1538–1542.
45. Botta A, Ramankutty N, Foley JA (2002) Long-term variations of climate and carbon fluxes over the Amazon basin. *Geophys Res Lett* 29(9):10–13.
46. Kim Y, et al. (2012) Seasonal carbon dynamics and water fluxes in an Amazon rainforest. *Glob Chang Biol* 18(4):1322–1334.
47. Asner GP, Townsend AR, Braswell BH (2000) Satellite observation of El Niño effects on Amazon Forest phenology and productivity. *Geophys Res Lett* 27(7):981–984.
48. Potter C, et al. (2001) Modeling seasonal and interannual variability in ecosystem carbon cycling for the Brazilian Amazon region. *J Geophys Res* 106(D10):10423–10446.
49. Lin JC, Matsui T, Pielke RA, Kummerow C (2006) Effects of biomass-burning-derived aerosols on precipitation and clouds in the Amazon Basin: A satellite-based empirical study. *J Geophys Res* 111:D19204.
50. Marengo JA (2004) Interdecadal variability and trends of rainfall across the Amazon basin. *Theoretical and Applied Climatology* 78(1-3):79–96.
51. Malhi Y, et al. (2008) Climate change, deforestation, and the fate of the Amazon. *Science* 319(5860):169–172.
52. Saatchi S, et al. (2013) Persistent effects of a severe drought on Amazonian forest canopy. *Proc Natl Acad Sci USA* 110(2):565–570.
53. Roy SB (2009) Mesoscale vegetation-atmosphere feedbacks in Amazonia. *J Geophys Res* 114:D20111.
54. Krishnaswamy J, John R, Joseph S (2014) Consistent response of vegetation dynamics to recent climate change in tropical mountain regions. *Glob Chang Biol* 20(1):203–215.
55. Bonan GB (2008) Forests and climate change: Forcings, feedbacks, and the climate benefits of forests. *Science* 320(5882):1444–1449.
56. Nobre CA, Sellers PJ, Shukla J (1991) Amazonian deforestation and regional climate change. *J Clim* 4(10):957–988.
57. Houghton RA, Lawrence KT, Hackler JL, Brown S (2008) The spatial distribution of forest biomass in the Brazilian Amazon: A comparison of estimates. *Glob Chang Biol* 7(7):731–746.
58. Zhao M, Running SW (2010) Drought-induced reduction in global terrestrial net primary production from 2000 through 2009. *Science* 329(5994):940–943.
59. Aragão LEOC, et al. (2007) Spatial patterns and fire response of recent Amazonian droughts. *Geophys Res Lett* 34:L07701.
60. Lyapustin A, et al. (2011) Multiangle implementation of atmospheric correction (MAIAC): 2. Aerosol algorithm. *J Geophys Res* 116:D03211.
61. Roujean JJ-L, Leroy M, Deschamps P-Y (1992) A bidirectional reflectance model of the Earth's surface for the correction of remote sensing data. *J Geophys Res* 97:20455–20468.
62. Lyapustin A, Wang Y, Frey R (2008) An automatic cloud mask algorithm based on time series of MODIS measurements. *J Geophys Res* 113:D16207.
63. Adler RF, Huffman GJ, Bolvin DT, Curtis S, Nelkin EJ (2000) Tropical rainfall distributions determined using TRMM combined with other satellite and rain gauge information. *J Appl Meteorol* 39(12):2007–2023.
64. Rodell M, et al. (2004) The global land data assimilation system. *Bull Am Meteorol Soc* 85(3):381–394.
65. Jönsson AM, Eklundh L, Hellström M, Bärring L, Jönsson P (2010) Annual changes in MODIS vegetation indices of Swedish coniferous forests in relation to snow dynamics and tree phenology. *Remote Sens Environ* 114:2719–2730.